La- and La-/Ce-Doped BaF_2 Crystals for Future HEP Experiments at the Energy and Intensity Frontiers Part I

Fan Yang, *Member, IEEE*, Junfeng Chen, *Member, IEEE*, Liyuan Zhang, *Member, IEEE*, Chen Hu, *Member, IEEE*, and Ren-Yuan Zhu, *Senior Member, IEEE*

***Abstract*—Because of its fast scintillation component with subnanosecond decay time, BaF_2 crystals are considered as a candidate for ultrafast crystal calorimeters for future high energy physics experiments at the energy and intensity frontiers. Undoped BaF_2, however, has a slow scintillation component with 600 ns decay time, which causes pile-up. In the part I of this paper, we report investigations on La doping in BaF_2 crystals to suppress the slow component. While typical fast/slow (F/S) ratio observed in undoped BaF_2 is 1/5, La-doped BaF_2 crystals were found to improve this ratio to about 1/1. The overall F/S ratio, however, is considered not sufficient for pile-up suppression.**

***Index Terms*—Barium fluoride, rare earth doping, slow scintillation component suppression.**

I. Introduction

BARIUM fluoride (BaF_2) crystals have a very fast scintillation component peaked at 220 nm with sub-nanosecond decay time, which provides a good foundation for an ultrafast calorimetry to face the challenge of the unprecedented high event rate expected in future high energy physics (HEP) experiments at the energy and intensity frontiers. BaF_2 was used to construct the two/three arm photon spectrometer (TAPS) calorimeter [1] and was proposed to build a precision electromagnetic calorimeter for Higgs searches at the proposed superconducting supercollider (SSC) back in the 90s [2]–[4]. It was also the baseline option for the Mu2e experiment at Fermilab [5]. BaF_2, however, has also a slow scintillation component peaked at 300 nm with 600 ns decay time and a five times intensity of the fast component, which leads to a serious pile-up effect [6]–[9]. It is thus crucial to suppress the slow component in BaF_2 for future high rate applications. Three approaches have been proposed: 1) selective doping with rare earth (La, Ce, and Y) or alkaline earth (Sr and Mg) [10]–[19]; 2) selective readout with solar blind photodetector, which is sensitive to the fast component while not to the slow component [8]; and 3) heating the crystal to reduce the slow component to about 1% of its initial value [20], [21].

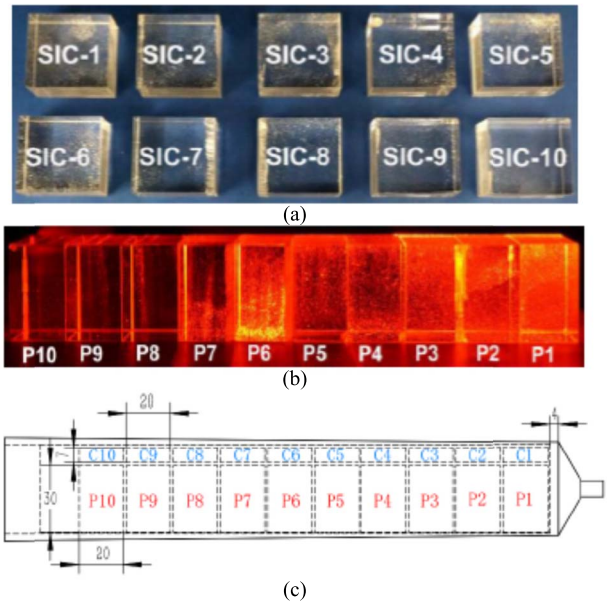

Fig. 1. (a) Photograph showing 10 La-doped samples. (b) These samples under illumination by a red LED. (c) Position of twenty samples in the La-doped ingot.

In the part I of this paper, we report investigations carried out at the Caltech HEP Crystal Lab for La-doped BaF_2 crystals grown at the Shanghai Institute of Ceramics (SIC). The part II of this paper will discuss La-/Ce co-doped BaF_2 crystals grown at the Beijing Glass Research Institute (BGRI), and makes a comparison. Our early result was presented in the Nuclear Science Symposium (NSS) 2016 conference [22].

II. Lanthanum-Doped BaF_2 Crystals

Early works pointed out that rare earth doping with, e.g., La, Ce, and Y suppresses the slow component in

Manuscript received October 29, 2018; accepted November 30, 2018. Date of publication December 5, 2018; date of current version January 17, 2019. This work was supported in part by the U.S. Department of Energy, Office of High Energy Physics program under Award DE-SC0011925, in part by the Fundamental Research Funds for the Central Universities of China, in part by the Natural Science Funds of China under Grant 51402332 and Grant 11775120, and in part by the Natural Science Funds of Tianjin under Grant 18JCYBJC17800. *(Corresponding author: Ren-Yuan Zhu.)*

F. Yang was with the HEP, California Institute of Technology, Pasadena, CA 91125 USA. He is now with the Key Laboratory of Weak-Light Nonlinear Photonics, Ministry of Education, School of Physics, Nankai University, Tianjin 300071, China (e-mail: fan@nankai.edu.cn).

J. Chen was with HEP, California Institute of Technology, Pasadena, CA 91125 USA. He is now with the Key Laboratory of Transparent Opto-Functional Inorganic Materials, Shanghai Institute of Ceramics, Chinese Academy of Sciences, Shanghai 201899, China (e-mail: jfchen@mail.sic.ac.cn).

L. Zhang, C. Hu, and R.-Y. Zhu are with the HEP, California Institute of Technology, Pasadena, CA 91125 USA (e-mail: zhu@hep.caltech.edu).

Color versions of one or more of the figures in this paper are available online at http://ieeexplore.ieee.org.

Digital Object Identifier 10.1109/TNS.2018.2884978

0018-9499 © 2018 IEEE. Personal use is permitted, but republication/redistribution requires IEEE permission.
See http://www.ieee.org/publications_standards/publications/rights/index.html for more information.

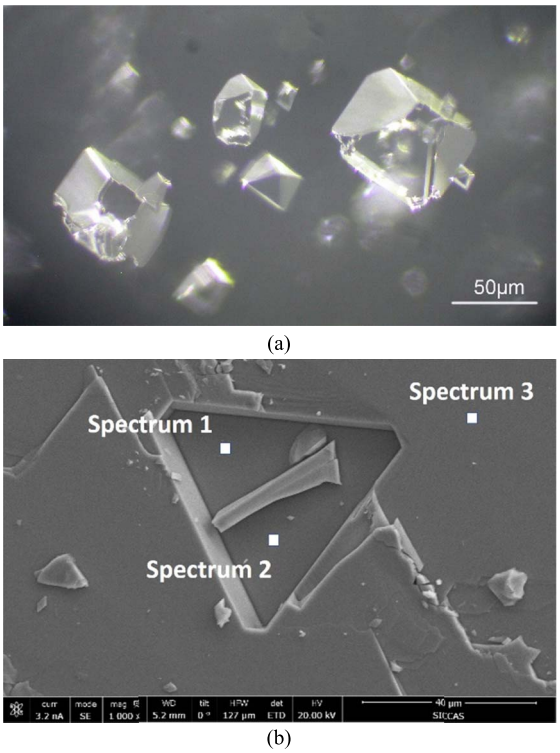

Fig. 2. Images of scattering centers observed by (a) optical microscopy and (b) SEM/EDS spectroscopy.

TABLE I

STOICHIOMETRIC RATIO OF SCATTERING CENTERS MEASURED BY SEM/EDS

	Concentration (wt%)		
	Ba	F	La
Spectrum 1	87.1	10.8	2.1
Spectrum 2	87.1	11.0	1.9
Spectrum 3	87.2	10.8	2.0

BaF_2 [11], [16]. Pure- and La-doped BaF_2 crystals were grown at SIC and were investigated at Caltech and SIC.

Fig. 1(a) shows 10 BaF_2 samples of $3 \times 3 \times 2$ cm^3 cut from a La-doped ingot. Fig. 1(b) shows these samples marked as P1 to P10 under a red LED illumination, revealing scattering centers in all samples with the most severe in the sample P6. Fig. 1(c) is the schematic showing locations of the samples P1–P10 in the ingot together with additional 10 samples of $3 \times 2 \times 0.7$ cm^3 marked as C1–C10 cut from the same ingot at the adjacent positions, respectively, to samples P1–P10.

Fig. 2 shows the images of scattering centers recorded by (a) an optical microscopy and (b) a scanning electron microscopy with energy dispersive spectroscopy (SEM/EDS). The scattering centers show octahedral, cubic, pentagonal-dodecahedron shape, or a combination of the above.

Table I shows consistent stoichiometric ratios measured by the SEM/EDS analysis for scattering centers (spectrums 1 and 2) and background (spectrum 3). This consistency indicates that the scattering centers are voids or bubbles, known as negative crystals formed according to the Roedder's liquid-inclusion formation mechanism [23]. While the shape and formation mechanism of negative crystal were investigated for pure BaF_2 crystals [24], its existence in La-doped BaF_2 crystals indicates a morphological instability of the solid–liquid interface during crystal growth. Such instability is caused by an out of controlled crystallization velocity, which occurs often at a high thermal gradient zone such as the seed end. To grow scattering center free crystals, the crystal growth parameters need to be further optimized.

TABLE II

CONCENTRATIONS OF LANTHANUM, CERIUM, AND LEAD IN PURE- AND La-DOPED SAMPLES

Sample ID.	Concentration (wt%)		
	La	Ce	Pb
Pure	<0.0004	<0.0007	<0.002
C1	0.993	<0.0007	<0.002
C2	0.999	<0.0007	<0.002
C3	1.074	<0.0007	<0.002
C4	0.999	<0.0007	<0.002
C5	0.979	<0.0007	<0.002
C6	0.945	<0.0007	<0.002
C7	0.855	<0.0007	<0.002
C8	0.831	<0.0007	<0.002
C9	0.766	<0.0007	<0.002
C10	0.951	<0.0007	<0.002

The concentrations of Ce, La, and Pb were measured by an Agilent 5100 synchronous vertical dual view (SVDV) inductively coupled plasma optical emission spectrometry (ICP-OES) at SIC. The calibrations were obtained by using a series of standards prepared from 1000 mg/L aqueous standards prepared at the Shanghai Institute of Measurement and Testing Technology. The statistical uncertainties of the trace analysis are 1% and 1.7% for La and Ce, respectively. The systematic uncertainty, caused by, e.g., scattering centers, is estimated to be at 5% level.

Table II lists the trace analysis results for La, Ce, and Pb in in the samples C1–C10, and compared to a pure sample. Pb was analyzed because PbF_2 serves as an oxygen scavenger in BaF_2 growth. While no trace element was found in the pure sample, the results show that both the Ce and Pb levels are below their detection limit of 7 and 20 ppm, respectively. The ICP-OES results also show that the La concentration increases slightly from C1 (the seed end) to C3, decreases from C3 to C9 (the tail end), and has an abnormal high in C10.

This La distribution can be explained by a relation suggested by Burton, Prim, and Slichter (BPS relation) [25]

$$C_s = C_0 k_{\text{eff}} (1-g)^{k_{\text{eff}}-1} \tag{1}$$

$$k_{\text{eff}} = \frac{k_0}{k_0 + (1-k_0)\exp\left(-\frac{\upsilon\delta}{D}\right)} \tag{2}$$

where C_s and C_0 are the dopants concentrations, respectively, in crystal and melt, g is the solidification fraction of the melt, and k_{eff} is the effective segregation coefficient. Here, ν is the crystallization velocity, D is the diffusion coefficient of dopants in melt, δ is the thickness of the diffusion limited boundary layer, and k_0 is the segregation coefficient with $\nu = 0$. According to the BPS relation, k_{eff} depends on

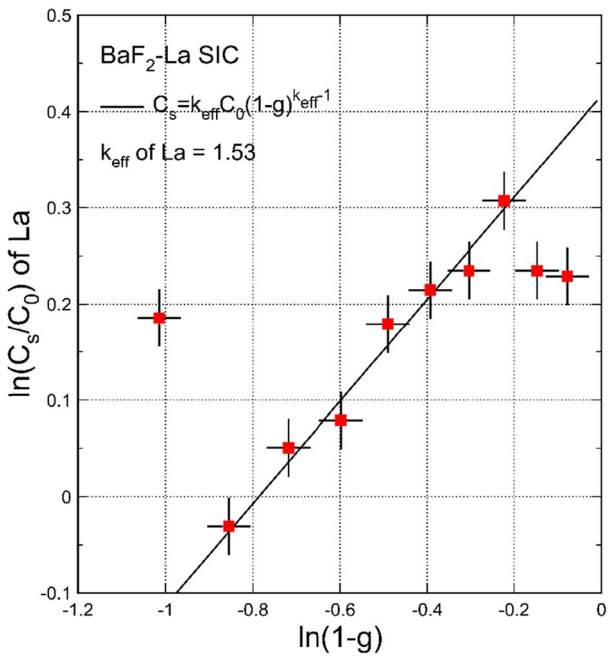

Fig. 3. Relative concentration of La as a function of solidification fraction.

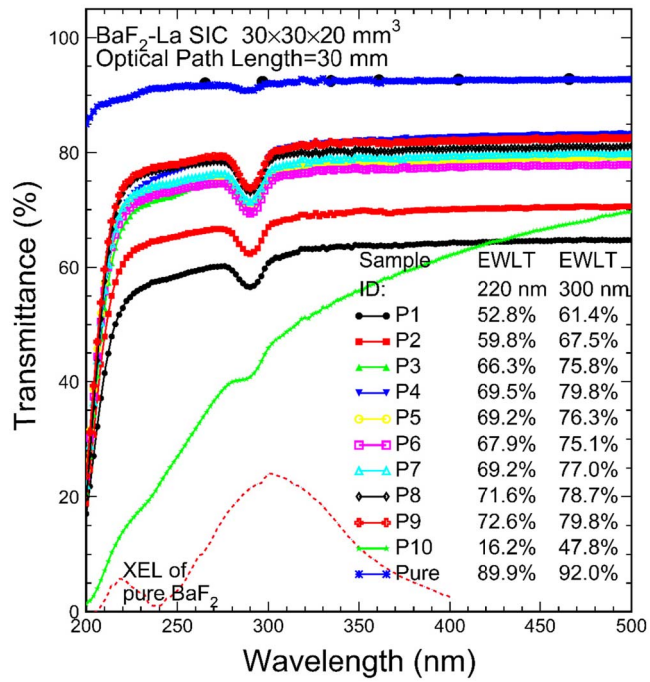

Fig. 4. Transmittance spectra of pure and La-doped BaF_2 samples.

the crystallization velocity. As discussed, the crystallization velocity is higher at the seed end, leading to a lower k_{eff}. This explains why the La concentration increases slightly from C1 (seed end) to C3, and then decreases from C3 to C9 (tail end). We also noticed an unplanned power outage during the growth of this ingot, which caused an incomplete growth. Consequently, the sample P10 is more like a frozen melt, where impurities were concentrated. We, therefore, used data from C3 to C9 to extract the effective segregation coefficient. Fig. 3 shows a linear fit, where the effective segregation coefficient for La in BaF_2 is determined to be 1.53 ± 0.09 for a crystal growth velocity of 2 mm/h.

Optical transmittance spectra were measured by using a PerkinElmer Lambda 950 spectrophotometer with 0.15% precision.

Fig. 4 shows the transmission spectra measured along 3 cm optical paths for 10 La-doped samples P1–P10 and compared to the pure sample. The black dots in Fig. 4 represent the theoretical limit of transmittance, which is calculated according to crystal's refractive index assuming no internal absorption [6]. Also shown in Fig. 4 is the X-ray excited luminescence (XEL) spectrum for pure BaF_2 and the numerical values of the emission weighted longitudinal transmittance (EWLT) for the fast (peaked at 220 nm) and slow (peaked at 300 nm) components, where EWLT is defined as

$$\text{EWLT} = \frac{\int LT(\lambda)\text{Em}(\lambda)d\lambda}{\int \text{Em}(\lambda)d\lambda}. \tag{3}$$

The EWLT values represent crystal's transparency for its scintillation light more accurately than the transmittance at the emission peak.

While the transmittance of pure BaF_2 approaches the theoretical limit between 275 and 500 nm, the transmittance of La-doped BaF_2 samples is much lower than the theoretical limit because of scattering centers in these samples. An unplanned power outage during the crystal growth caused an uncompleted growth. Consequently, the sample P10 is more like the frozen melt than crystal, where the impurities were concentrated causing the worst transmittance. It explains the abnormal transmittance observed in the sample P10.

Two absorption bands peaked at 204 and 290 nm are observed in all La-doped samples. The 204 nm absorption band reduces the fast component peaked at 220 nm, so is harmful for the overall fast/slow (F/S) ratio, which is defined as the ratio between the amounts of the fast and slow scintillation light observed by the photodetector. An early work attributes the 290 nm absorption band to Ce contamination introduced during La doping [12]. Although the ICP-OES result shows that Ce concentration is less than 7 ppm, it is suspected that the residual Ce level below 7 ppm may cause this absorption since a 290 nm excitation band of Ce was also observed in photoluminescence (PL) spectra in this La-doped BaF_2 sample. Another possibility is some undetected impurities, e.g., oxygen contamination introduced during the growth process. Further investigations are needed to understand the nature of this absorption. For such investigation, samples free from scattering centers are needed. XEL spectra were measured by using an FLS920 fluorescence spectrophotometer. Fig. 5 shows the setup, where samples were excited by X-rays from an X-ray tube.

XEL spectrum was measured in a reflection mode, so that only the scintillation light from sample's surface was collected. This light collection mode minimizes the effect of absorption within the sample bulk [26], so is not sensitive to sample's optical quality or transparency. The FLS920 fluorescence spectrophotometer was calibrated by using calibrated light sources.

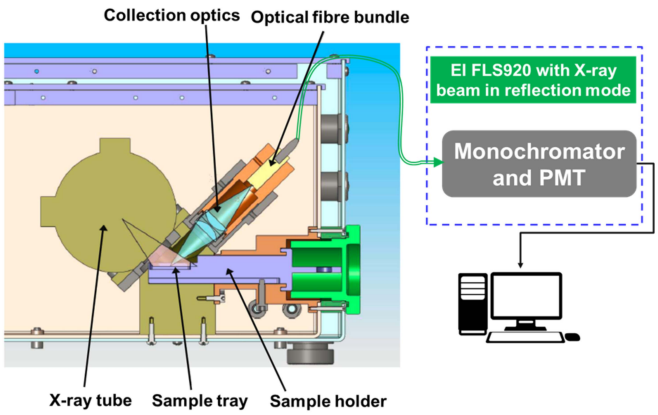

Fig. 5. Setup of XEL measurement by using FLS920 spectrometer.

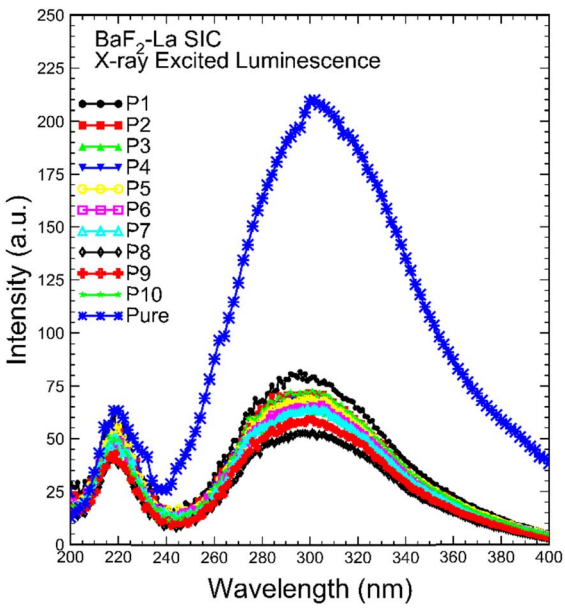

Fig. 6. Comparison of XEL spectra for pure and La-doped BaF_2.

Fig. 6 shows the XEL spectra measured for one pure and 10 La-doped BaF_2 samples. Consistent emission bands peaked at 220 and 300 nm are observed in all samples, indicating that La doping does not introduce new scintillation centers in BaF_2. Compared to pure BaF_2, however, both the fast and the slow scintillation are reduced. While the reduction of the slow component is significant, it is minor for the fast component.

The reduction of the fast component is attributed to a slightly reduced efficiency of the cross-luminescence in La-doped BaF_2. The reduction of the slow component is attributed to the quenching centers introduced by the La doping, which leads to nonradiative decays of self-trapped excitons (STE) of the slow component [27]. The trivalent rare earth ions (La^{3+}) replace Ba^{2+} ions in the lattice, leading to a charge imbalance. The overall charge is balanced by defects, such as interstitial F^- complexes or O^- centers due to oxygen contamination. These defects may act as quenching centers. The phenomenon has been observed in several trivalent rare earth (La, Ce, and Y)-doped BaF_2 crystals [10], [12], [13], [17], [28], [29].

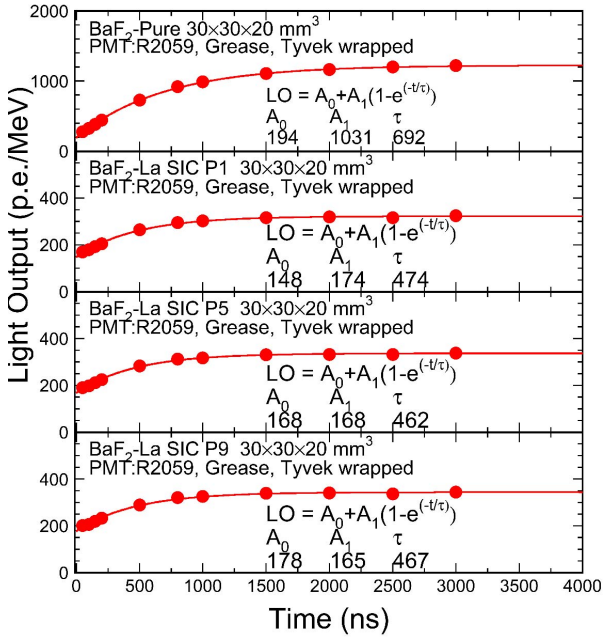

Fig. 7. LO is shown as a function of integration time for pure and La-doped BaF_2 samples excited by γ-rays.

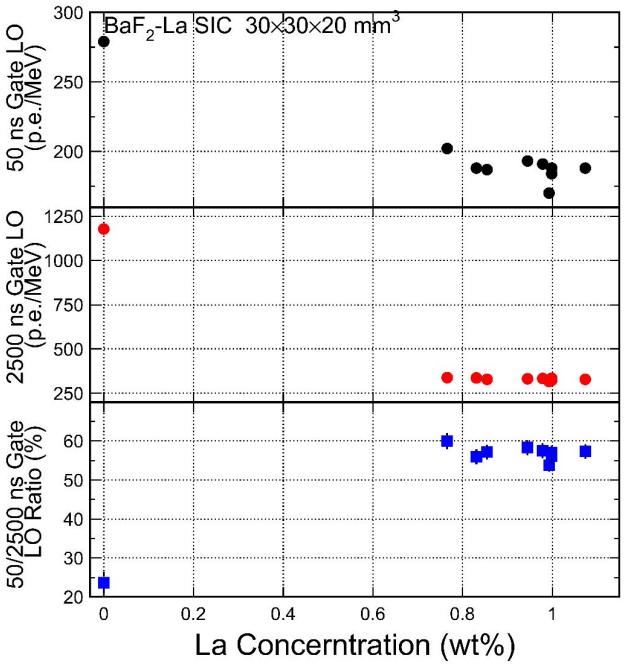

Fig. 8. LO in 50 (top) and 2500 ns (middle) and their ratio (bottom) are shown as a function of the La concentration for a pure and nine La-doped BaF_2 samples.

Light output (LO) and decay kinetics were measured by a Hamamatsu R2059 PMT with a grease coupling for 0.511 MeV γ-rays from a Na-22 source with a coincidence trigger. The scintillation light collected by a Hamamatsu R2059 PMT was integrated by a LeCroy 3001 QVT in the Q mode. The integration gates were provided by a LeCroy 2323A

gate generator. The light output was calibrated with single photoelectron peaks with systematic uncertainties of 1% [30].

Fig. 7 shows the LO as a function of integration time for one pure and three La-doped BaF_2 samples. Significant reduction in both LO and decay time is observed in La-doped BaF_2 samples as compared to the pure sample. The reduction of the slow component is much more than the fast component, which is consistent with what observed in the XEL spectra. The overall F/S ratio, obtained as A_0/A_1 from the fit, shows an improvement from 1/5 for pure BaF_2 up to 1/1 for La-doped BaF_2 crystals.

Fig. 8 shows LO in 50 (top) and 2500 ns (middle) and their ratio (bottom) as a function of the La concentration in the pure and nine La-doped (P1 to P9) BaF_2 samples.

Both the fast and slow components are reduced by the La doping. The fast/total (F/T) ratio, defined as the ratio between the LO of 50 and 2500 ns gates, is increased from 1/6 for pure BaF_2 up to about 3/5 for La-doped BaF_2, corresponds to an increase of the F/S ratio from 1/5 to 1/1. The results of this investigation are consistent with early reports by Schotanus *et al*. [10] and Woody *et al*. [11].

We also note the LO in 50 ns gate decreases slightly as the La concentration increases from 0.76 to 1.07 wt%, while there are no obvious variations in the LO of 2500 ns, indicating that the optimized La concentration level in BaF_2 is less than 0.76 wt%.

III. Conclusion

The ultrafast scintillation light with sub-nanometer decay time in BaF_2 crystals provides sufficient light output for ultrafast calorimeters. The issue of BaF_2 crystal's slow scintillation light with 600 ns decay time can be handled by several approaches: selective doping, selective readout with solar blind photodetector or heating the crystal.

La-doped BaF_2 crystals were grown at SIC and were investigated at Caltech. They show relatively poor optical quality caused by negative crystal defects, indicating that the crystal growth parameters need to be further optimized. The distribution of La in BaF_2 crystals was analyzed by ICP-OES, and was used to extract the effective segregation coefficients 1.53 ± 0.09 at a crystallization velocity of 2 mm/h.

La doping in the BaF_2 reduces light output of the slow component more than the fast component. The slow suppression of the La doping is due to quenching centers for the slow STE light. Consequently, the F/S ratio in the La doping crystal is improved from 1/5 to 1/1, consistent with previous publications. Such a suppression, however, is judged to be not sufficient for the Mu2e experiment to mitigate the pile-up effect.

In the part II, we will report our investigations on La/Ce co-doped BaF_2 crystals grown at BGRI as well as a comparison between La doping and La/Ce co-doping.

Acknowledgment

The authors would like to thank the Mu2e collaboration for providing funds to procure the BaF_2 samples discussed in this paper as well as many useful discussions.

References

[1] R. Novotny, "The BaF_2 photon spectrometer TAPS," *IEEE Trans. Nucl. Sci.*, vol. 38, no. 2, pp. 379–385, Apr. 1991.
[2] R. Y. Zhu, document GEM TN-91-32 and CALT 68-1777, 1991.
[3] R. Y. Zhu and H. Yamammoto, document GEM TN-92-126 and CALT 68-1802, 1992.
[4] S. Mrenna, S. Shevchenko, X. R. Shi, H. Yamamoto, and R. Y. Zhu, document GEM TN-93-373 and CALT 68-1856, 1993.
[5] G. Pezzullo *et al.*, "The LYSO crystal calorimeter for the Mu2e experiment," *J. Instrum.*, vol. 9, p. C03018, Mar. 2014.
[6] D.-A. Ma and R.-Y. Zhu, "Light attenuation length of barium fluoride crystals," *Nucl. Instrum. Methods Phys. Res. A, Accel. Spectrom. Detect. Assoc. Equip.*, vol. 333, pp. 422–424, Sep. 1993.
[7] M. Laval *et al.*, "Barium fluoride—Inorganic scintillator for subnanosecond timing," *Nucl. Instrum. Methods Phys. Res.*, vol. 206, pp. 169–176, Feb. 1983.
[8] R.-Y. Zhu, "On quality requirements to the barium fluoride crystals," *Nucl. Instrum. Methods Phys. Res. A, Accel. Spectrom. Detect. Assoc. Equip.*, vol. 340, pp. 442–457, Mar. 1994.
[9] Z. Y. Wei, R. Y. Zhu, H. Newman, and Z. W. Yin, "Light yield and surface treatment of barium fluoride crystals," *Nucl. Instrum. Methods Phys. Res. B, Beam Interact. Mater. At.*, vol. 61, pp. 61–66, Jul. 1991.
[10] P. Schotanus, P. Dorenbos, C. W. E. van Eijk, and H. J. Lamfers, "Suppression of the slow scintillation light output of BaF_2 crystals by La^{3+} doping," *Nucl. Instrum. Methods Phys. Res. A, Accel. Spectrom. Detect. Assoc. Equip.*, vol. 281, pp. 162–166, Aug. 1989.
[11] C. L. Woody, P. W. Levy, and J. A. Kierstead, "Slow component suppression and radiation-damage in doped BaF_2 crystals," *IEEE Trans. Nucl. Sci.*, vol. 36, no. 1, pp. 536–542, Feb. 1989.
[12] P. Dorenbos, R. Visser, R. W. Hollander, C. W. E. van Eijk, and H. W. Den Hartog, "The effects of La^{3+} and Ce^{3+} dopants on the scintillation properties of BaF_2 crystals," *Radiat. Effects Defects Solids*, vols. 119–121, no. 1, pp. 87–92, 1991.
[13] R. Visser, P. Dorenbos, C. W. E. van Eijk, R. W. Hollander, and P. Schotanus, "Scintillation properties of Ce^{3+} doped BaF_2 crystals," *IEEE Trans. Nucl. Sci.*, vol. 38, no. 2, pp. 178–183, Apr. 1991.
[14] P. Dorenbos, R. Visser, R. Dool, J. Andriessen, and C. W. E. van Eijk, "Suppression of self-trapped exciton luminescence in La^{3+}- and Nd^{3+} -doped BaF_2," *J. Phys., Condens. Matter*, vol. 4, no. 23, p. 5281, 1992.
[15] M. M. Hamada, Y. Nunoya, S. Sakuragui, and S. Kubota, "Suppression of the slow component of BaF_2 crystal by introduction of SrF_2 and MgF_2 crystals," *Nucl. Instrum. Methods Phys. Res. A, Accel. Spectrom. Detect. Assoc. Equip.*, vol. 353, pp. 33–36, Dec. 1994.
[16] B. P. Sobolev, E. A. Krivandina, S. E. Derenzo, W. W. Moses, and A. C. West, "Suppression of BaF_2 slow component of X-RAY luminescence in non-stoichiometric $Ba_{0.9}R_{0.1}F_{2.1}$ crystals (R=rare earth element)," *Proc. Mater. Res. Soc., Scintillator Phosphor Mater*, vol. 348, pp. 277–283, Feb. 1994.
[17] W. Drozdowski, K. R. Przęgietka, A. J. Wojtowicz, and H. L. Oczkowski, "Charge traps in Ce-doped CaF_2 and BaF_2," *Acta Phys. Polonica A*, vol. 95, no. 2, pp. 251–258, 1999.
[18] V. Trnovcová, N. I. Sorokin, P. P. Fedorov, E. A. Krivandina, T. Srámková, and B. P. Sobolev, "Electrical properties of heavily doped fluorite-structured BaF_2: RF_3 (R=La, Pr, Nd, Gd, Tb, Y, Sc) single crystals," *Ionics*, vol. 6, pp. 351–358, Sep. 2000.
[19] V. Nesterkina, N. Shiran, A. Gektin, K. Shimamura, and E. Villora, "The Lu-doping effect on the emission and the coloration of pure and Ce-doped BaF_2 crystals," *Radiat. Meas.*, vol. 42, pp. 819–822, Apr./May 2007.
[20] M. Biasini, D. B. Cassidy, S. H. M. Deng, H. K. M. Tanaka, and A. P. Mills, "Suppression of the slow component of scintillation light in BaF_2," *Nucl. Instrum. Methods Phys. Res. A, Accel. Spectrom. Detect. Assoc. Equip.*, vol. 553, pp. 550–558, Nov. 2005.
[21] P. Schotanus, C. W. E. van Eijk, R. W. Hollander, and J. Pijpelink, "Temperature dependence of BaF_2 scintillation light yield," *Nucl. Instrum. Methods Phys. Res. A, Accel. Spectrom. Detect. Assoc. Equip.*, vol. 238, pp. 564–565, Aug. 1985.
[22] F. Yang, J. Chen, L. Zhang, and R. Zhu, "Development of BaF_2 crystals for future HEP experiments at the intensity frontiers," in *Proc. IEEE Nucl. Sci. Symp., Med. Imag. Conf. Room-Temp. Semiconductor Detect. Workshop (NSS/MIC/RTSD)*, Oct./Nov. 2016, pp. 1–4.
[23] U. Petersen, "Geochemistry of hydrothermal ore deposits. Hubert Lloyd Barnes," *J. Geol.*, vol. 76, p. 606, Sep. 1968.
[24] S. Hua and W. Zhong, "Crystallization habit and defect of BaF_2," *J. Synth. Cryst.*, vol. 21, no. 2, pp. 131–136, 1992.

[25] J. A. Burton, R. C. Prim, and W. P. Slichter, "The distribution of solute in crystals grown from the melt—Part I: Theoretical," *J. Chem. Phys.*, vol. 21, no. 11, pp. 1987–1991, 1953.

[26] R. Mao, L. Zhang, and R.-Y. Zhu, "Emission spectra of LSO and LYSO crystals excited by UV light, X-ray and γ-ray," *IEEE Trans. Nucl. Sci.*, vol. 55, no. 3, pp. 1759–1766, Jun. 2008.

[27] R. Visser, P. Dorenbos, C. W. E. van Eijk, and H. W. den Hartog, "Energy transfer processes observed in the scintillation decay of BaF_2: La," *J. Phys., Condens. Matter*, vol. 4, no. 45, p. 8801, 1992.

[28] R.-Y. Zhu, "Very fast inorganic crystal scintillators," *Proc. SPIE*, vol. 10392, p. 103920G, Sep. 2017.

[29] J. Chen *et al.*, "Slow scintillation suppression in yttrium doped BaF_2 crystals," *IEEE Trans. Nucl. Sci.*, vol. 65, no. 8, pp. 2147–2151, Aug. 2018.

[30] R. Mao, L. Zhang, and R. Y. Zhu, "Optical and scintillation properties of inorganic scintillators in high energy physics," *IEEE Trans. Nucl. Sci.*, vol. 55, no. 4, pp. 2425–2431, Aug. 2008.